Theoret.Appl.Mech. TEOPM7,Vol.40, No.2, pp.203–221, Belgrade 2013*

ACTIVE CONTROL OF MECHANICAL STRUCTURES IN RESEARCH AND EDUCATION

Tamara N. Nestorović

*doi: 10.2298/TAM1302203N Math.Subj.Class.: 93C40; 93B03; 93C10; 74S05;

According to: *Tib Journal Abbreviations (C) Mathematical Reviews*, the abbreviation TEOPM7 stands for TEORIJSKA I PRIMENJENA MEHANIKA.

THEORETICAL AND APPLIED MECHANICS
Series: **Special Issue - Address to Mechanics, Vol. 40 (S1), pp. 203-221, Belgrade 2012.**

ACTIVE CONTROL OF MECHANICAL STRUCTURES IN RESEARCH AND EDUCATION

UDC 531.2; 531.146; 531.8.

Tamara N. Nestorović

Ruhr-Universität Bochum, AG Mechanik adaptiver Systeme
Universitätsstraße 150, Geb. IA-01/128, D-44801 Bochum, Germany

Abstract. *Several crucial phases of the overall approach to development and design of smart structures are outlined in this paper. They are focused on control of lightweight mechanical structures with respect to active vibration and noise attenuation using piezoelectric actuators and sensors. The research experience and growing interest in development of smart structures have motivated introduction of courses on smart structures at universities, which are being studied extensively and with great interest by young researchers and students. Some of the author's experiences regarding education in this field will be addressed as well.*

Key words: *active structural control, piezoelectric actuators and sensors, system identification.*

1. INTRODUCTION

Active structural control has been intensively investigated in the recent years. It is not only a subject of the scientific and research activities, but due to its extensive application possibilities active control of mechanical structures gains more and more attention in the education and teaching processes. In that way the benefits of the further development and application can be recognized in the early stages, awaking the interest among young future experts to investigate and contribute more in this field.

In this paper a broad field of active structural control is considered within the focused frame regarding control of lightweight mechanical structures with respect to active vibration and noise attenuation using piezoelectric actuators and sensors. An overall approach to active control of piezoelectric structures involves subsequent steps of modeling, control, simulation, experimental verification and implementation. Each of these steps is regarded in more details. Numerical modeling is regarded from the finite element method (FEM) point of view [5–6, 11]. Parameter identification [13, 15, 19] is considered as a complementary approach to obtain representative models for the use in subsequent development steps, e.g. controller design. Active controller design involves optimal [16] and adaptive methods [14], whereas the simulation and verification methods

involve consideration of the real-time applications. Some application examples[3] showing the feasibility of the active structural control are presented (vibration suppression of the car roof, active noise control of the acoustic box).

Studying of active structural control is involved in education and teaching processes at the high-school level as well. This topic addresses especially teaching experiences in the field of adaptronics, mechatronics, mechanics of adaptive systems and control theory.

As an introduction an example of actively controlled vibrations of a clamped beam is explained as a benchmark example presented at the courses on active structural control and mechatronics for the students involved in higher education phases. Subsequently the overall development of smart structures is summarized and illustrated by several application examples.

2. ACTIVE VIBRATION CONTROL OF A CANTILEVER BEAM – AN EDUCATIONAL AND RESEARCH BENCHMARK EXAMPLE

Many scientific and practical, but also educational experiences can be gained by investigation of a clamped beam problem. In this section an overall approach to the vibration suppression of a clamped beam excited at the tip will be described. This example represents a valuable contribution to the educational process, since the vibration control problem formulation and its solution defined in several subsequent logical steps follow the overall approach to smart structures analysis and design procedure and therefore apply as a standard procedure in investigation and control of much more complex smart structures. On the other hand, the problem retains the scientific complexity and opens possibilities for further studies and contributions to the improvement of the problem solution.

The investigated clamped beam is considered as an active plate structure controlled by four piezoelectric patch actuators attached to the beam, two on the top and two on the bottom of the plate. Geometry of a standard beam including piezo patches as actuators and/or sensor is represented in Fig.1. The material properties of the beam and piezo electric material are listed in Table 1. In the first step the plant was represented in the form of a finite element model with a mesh of 235 passive and 80 active Semiloof shell elements [2, 5]. On the basis of this mesh the eigenfrequencies and eigenmodes are calculated using a numerical procedure supported by some standard finite element software. The eigenmodes can be determined experimentally as well, using the modal analysis approach. The eigenfrequencies of interest for bending mode case studies are considered in the subsequent investigations. Exciting forces $F(t)=A\sin(\omega_i t)$ exerted on the corner points at the tip of the beam are chosen with regard to the eigenfrequencies of interest.

An experimental rig with the clamped cantilever beam and dSPACE system, which can be used for the modal analysis and control purposes, is shown in Fig. 2.

[3] Experimental studies and application examples addressed in this paper were performed within the author's research activities at the Otto-von-Guericke University of Magdeburg, Germany, supported by Prof. Dr.-Ing. habil. Ulrich Gabbert and the research group at the Institute of Mechanics. This support is greatly acklnowledged.

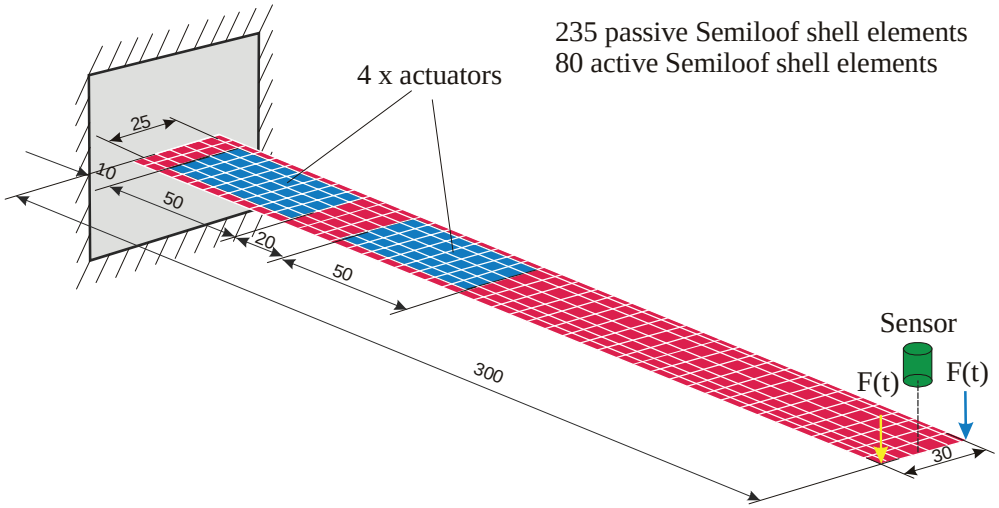

Fig. 1 Geometry and dimensions of the clamped beam with finite element mesh

Table 1. Material properties

Beam	$E = 2.00 \cdot 10^5$ N/mm^2	Piezo	$E_{11} = E_{22} = 3.77 \cdot 10^4$N/mm^2
	$\nu = 0.3$		$G_{12} = 1.3 \cdot 10^4$ N/mm^2
	$\rho = 7.86 \cdot 10^{-9}$ Ns^2/mm^4		$\nu = 0.38$
	t = 2.0 mm (thickness)		$\rho = 7.85 \cdot 10^{-9}$ Ns^2/mm^4
			$d_{31} = 2.1 \cdot 10^{-7}$ mm/V
			$\kappa_{33} = 3.36 \cdot 10^{-9}$ F/m
			$\rho = 7.85 \cdot 10^{-9}$ Ns^2/mm^4

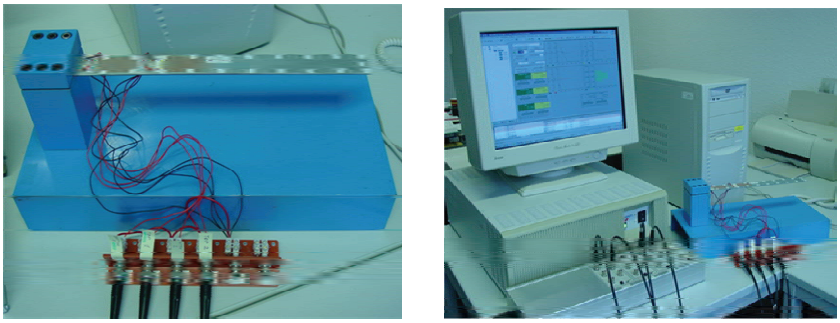

Fig. 2 Experimental rig with the clamped cantilever beam and dSPACE system

Control problem can be formulated as schematically represented in the Fig. 3. For the solution of the control task an appropriate controller is proposed (optimal LQ controller) in the way that the vibration amplitudes due to periodic excitation forces with frequencies

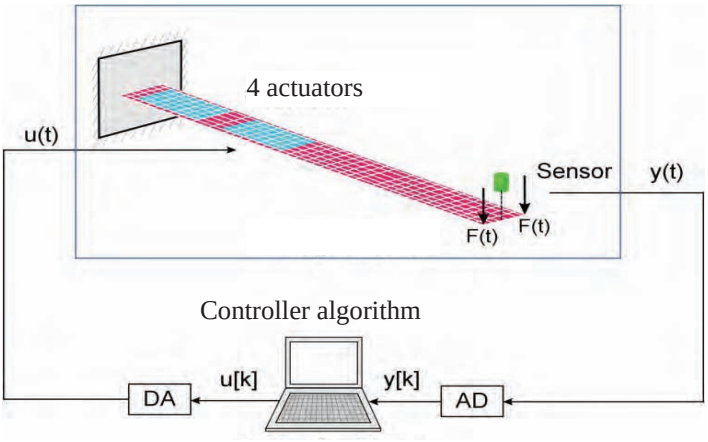

Fig. 3 Closed-loop control system for the vibration suppression of the clamped beam

corresponding to the eigenfrequencies of the clamped beam, are significantly suppressed in comparison with uncontrolled case. The study of the control problem is enabled through the simulations which are performed using the Matlab/Simulink software. As a starting point for the controller design an appropriate state space model was developed, based on the modal truncation of the finite element model of a much higher order, in such a way that the modally reduced state space model contains important information on the eigenmodes in the frequency range of interest, in this case: f_1=18.8Hz, f_2=113.1Hz, f_3=314.4Hz, f_6=619.2Hz (the eigenmodes 4 and 5 are torsion modes, and they are not relevant for the bending vibration suppression). The results of the bending modes animation preceding the state space modal truncation are represented in Fig. 4.

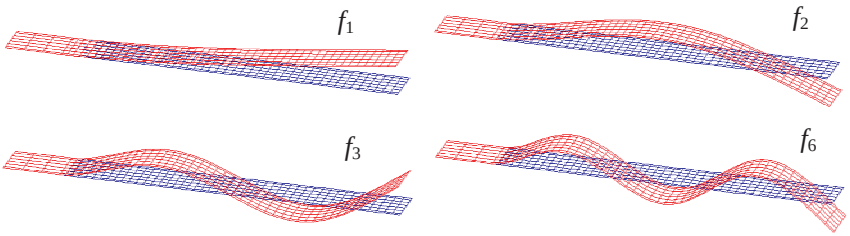

Fig. 4 Bending modes of the clamped beam

Simulation of the controller behavior is performed in Simulink using a block diagram with the optimal LQ controller and with an observer for unmeasurable state variables (Fig. 5).

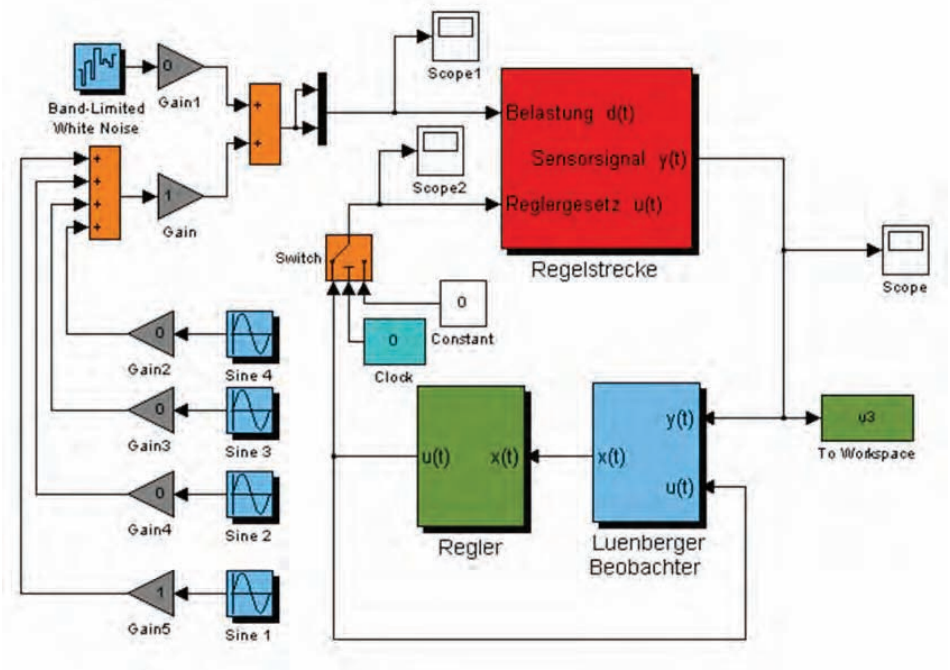

Fig. 5 Simulink block diagram for the simulation of the controlled beam behavior

Controller design results and its effects are shown in the diagrams in Fig. 6 represented the uncontrolled and controlled (after 0.5 s) output – displacement at the tip of the beam, as well as the control signals (actuating voltages on the piezo patches) without and with control.

Presented example illustrates in a comprehensive way the most important phases of system modeling, analysis, controller design, simulation and verification. Analytic and detailed study of the system behavior is possible based on the developed system model. In this way an overall view of the smart structures development can be gained using a relatively simple and comprehensive benchmark example, which plays an important role in educational process. On the other hand, the knowledge gained through the investigation of such examples can be successfully used for studying of more complex structures.

In subsequent sections an overall view of the most important phases in design and control of lightweight smart structures with piezoelectric active materials will be summarized and illustrated by several application examples.

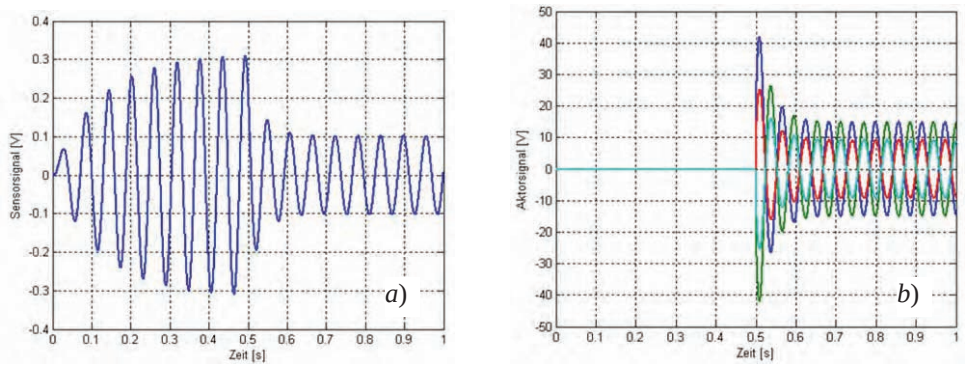

Fig. 6 Signals without control (up to 0.5 s) and with control (after 0.5s).
a) Controlled output. *b*) Actuating inputs.

3. FINITE ELEMENT APPROACH TO MODELING OF SMART STRUCTURES

The finite element (FE) based modeling of piezoelectric adaptive smart systems and structures represents a good basis for the overall simulation and design. This approach enables both a suitable controller design [14, 16] and the appropriate actuator/sensor placement [2, 8].

The FE analysis is based on the finite element semi-discrete form of the equations of motion of a piezoelectric smart system describing its electro-mechanical behavior. These equations can be derived using the established approximation method of displacements and electric potential and the standard finite element procedure [7, 9]. Here the coupled electro-mechanical behavior of smart structures will be considered. For investigations in the field of active acoustic modeling and control, appropriate consideration of the acoustic fluid is required. More on acoustic modeling can be found in [11].

Constitutive equations in the stress-charge form (1) are used for the development of the equations of motion for a smart structure:

$$\boldsymbol{\sigma} = \mathbf{C}\boldsymbol{\varepsilon} - \mathbf{e}\mathbf{E}, \qquad \mathbf{D} = \mathbf{e}^{\mathrm{T}}\boldsymbol{\varepsilon} + \boldsymbol{\kappa}\mathbf{E} \tag{1}$$

with following notations: $\boldsymbol{\sigma}^{\mathrm{T}} = \left[\sigma_{11} \quad \sigma_{22} \quad \sigma_{33} \quad \sigma_{12} \quad \sigma_{23} \quad \sigma_{31}\right]$ mechanical stress vector, $\mathbf{C}_{(6\times6)}$ symmetric elasticity matrix, $\boldsymbol{\varepsilon}^{\mathrm{T}} = \left[\varepsilon_{11} \quad \varepsilon_{22} \quad \varepsilon_{33} \quad 2\varepsilon_{12} \quad 2\varepsilon_{23} \quad 2\varepsilon_{31}\right]$ strain vector, $\mathbf{E}^{\mathrm{T}} = \left[E_1 \quad E_2 \quad E_3\right]$ electric field vector, $\mathbf{e}_{(6\times3)}$ piezoelectric matrix, $\mathbf{D}^{\mathrm{T}} = \left[D_1 \quad D_2 \quad D_3\right]$ vector of electrical displacement and $\boldsymbol{\kappa}_{(3\times3)}$ symmetric dielectric matrix. The system of equations which describe electromechanical behaviour consists of the constitutive equations (1) together with the mechanical equilibrium and electric equilibrium (charge equation of electrostatics resulting from the 4$^{\mathrm{th}}$ Maxwell equation):

$$\mathbf{D}_u^{\mathrm{T}}\boldsymbol{\sigma} + \mathbf{P} - \rho\mathbf{v} = \mathbf{0}, \quad \mathbf{D}_\varphi^{\mathrm{T}}\mathbf{D} = \mathbf{0} \tag{2}$$

where $\mathbf{P}^{\mathrm{T}} = \begin{bmatrix} P_1 & P_2 & P_3 \end{bmatrix}$ represents the body force vector, $\mathbf{v}^{\mathrm{T}} = \begin{bmatrix} v_1 & v_2 & v_3 \end{bmatrix}$ is the vector of mechanical displacements, ρ is the mass density and $\mathbf{D}_u$ and $\mathbf{D}_\phi$ are differentiation matrices:

$$\mathbf{D}_u^{\mathrm{T}} = \begin{bmatrix} \dfrac{\partial}{\partial x_1} & 0 & 0 & \dfrac{\partial}{\partial x_2} & 0 & \dfrac{\partial}{\partial x_3} \\ 0 & \dfrac{\partial}{\partial x_2} & 0 & \dfrac{\partial}{\partial x_1} & \dfrac{\partial}{\partial x_3} & 0 \\ 0 & 0 & \dfrac{\partial}{\partial x_3} & 0 & \dfrac{\partial}{\partial x_2} & \dfrac{\partial}{\partial x_1} \end{bmatrix}, \quad \mathbf{D}_\varphi^{\mathrm{T}} = \begin{bmatrix} \dfrac{\partial}{\partial x_1} & \dfrac{\partial}{\partial x_2} & \dfrac{\partial}{\partial x_2} \end{bmatrix}. \tag{3}$$

Variational statement of the governing equations for the coupled electro-mechanical problem derived from the Hamilton's principle represents the basis for development of the finite element model [1, 17–18]. It is obtained in the form:

$$\begin{aligned} &-\int_V \left(\rho\,\delta\mathbf{v}^{\mathrm{T}}\ddot{\mathbf{v}} - \delta\boldsymbol{\varepsilon}^{\mathrm{T}}\mathbf{C}\boldsymbol{\varepsilon} + \delta\boldsymbol{\varepsilon}^{\mathrm{T}}\mathbf{e}^{\mathrm{T}}\mathbf{E} \right) dV + \int_V \left(\delta\mathbf{E}^{\mathrm{T}}\mathbf{e}\boldsymbol{\varepsilon} + \delta\mathbf{E}^{\mathrm{T}}\boldsymbol{\kappa}\mathbf{E} + \delta\mathbf{v}^{\mathrm{T}}\mathbf{F}_{\mathrm{V}} \right) dV \\ &+ \int_{\Omega_1} \delta\mathbf{v}^{\mathrm{T}}\mathbf{F}_{\Omega}\, d\Omega + \delta\mathbf{v}^{\mathrm{T}}\mathbf{F}_{\mathrm{P}} - \int_{\Omega_2} \delta\varphi\, q\, d\Omega - \delta\varphi\, Q = 0 \end{aligned} \tag{4}$$

where F_Ω represents the surface applied forces (defined on surface Ω_1), F_P the point loads, ϕ the electric potential, q the surface charge brought on surface Ω_2 and Q the applied concentrated electric charges. Applying the approximation of displacements and electric potential with the shape functions over an element, representing the structure by a finite number of elements and adding up all elements contributions, the finite element semi-discrete form of the equations of motion is obtained:

$$\mathbf{M}\ddot{\mathbf{q}} + \mathbf{D}_d\dot{\mathbf{q}} + \mathbf{K}\mathbf{q} = \bar{\mathbf{E}}\mathbf{f}(t) + \bar{\mathbf{B}}\mathbf{u}(t) \tag{5}$$

where vector $\mathbf{q}$ represents the vector of generalized displacements including mechanical displacements and electric potential and contains all degrees of freedom. Matrices $\mathbf{M}$, $\mathbf{D}_d$ and $\mathbf{K}$ are the mass matrix, the damping matrix and the stiffness matrix, respectively. The total load vector is divided into the vector of the external forces $\mathbf{F}_E = \bar{\mathbf{E}}\mathbf{f}(t)$ and the vector of the control forces $\mathbf{F}_C = \bar{\mathbf{B}}\mathbf{u}(t)$, where the forces are generalized quantities including also electric charges. Vector $\mathbf{f}(t)$ represents the vector of external disturbances, and $\mathbf{u}(t)$ is the vector of the controller influence on the structure. Matrices $\bar{\mathbf{E}}$ and $\bar{\mathbf{B}}$ describe the positions of the forces and the control parameters in the finite element structure, respectively.

This approach has been used to develop a comprehensive library of multi-field finite elements: 1D, 2D, 3D elements, thick and thin layered composite shell elements, etc. which was implemented in the finite element package COSAR [3] for the simulation of the static and dynamic structural behavior of smart structures. Besides, the tools which take into account other physical effects are also available. For example, the temperature

influence can also be considered, and using the developed acoustic elements the influence of the acoustic fluid and its behavior can also be studied [10, 11].

The tools for modal reduction are also included, which enable development of appropriate models with reduced orders for the controller design. Based on the modal truncation, which was adopted as a suitable technique for the reduction of the number of equations in the FE models, a state space model of an actively controlled structure can be obtained in the form convenient for the controller design. A limited number of eigenmodes of interest is taken into account, while the remaining modes are truncated. Introducing the modal coordinates $\mathbf{z}$

$$\mathbf{q}(t) = \mathbf{\Phi}_{\mathrm{m}}\mathbf{z}(t) \tag{6}$$

into equation (5), where $\mathbf{\Phi}_{\mathrm{m}}$ represents the modal matrix, and applying the orthonormalization with $\mathbf{\Phi}_{\mathrm{m}}^{\mathrm{T}}\mathbf{M}\mathbf{\Phi}_{\mathrm{m}} = \mathbf{I}$, $\mathbf{\Phi}_{\mathrm{m}}^{\mathrm{T}}\mathbf{K}\mathbf{\Phi}_{\mathrm{m}} = \mathbf{\Omega}$, $\mathbf{\Delta} = \mathbf{\Phi}_{\mathrm{m}}^{\mathrm{T}}\mathbf{D}_{\mathrm{d}}\mathbf{\Phi}_{\mathrm{m}}$, where $\mathbf{\Omega}$ represents the spectral matrix and $\mathbf{\Delta}$ the modal damping matrix, the state space model of the modally reduced system can be obtained in the form:

$$\dot{\mathbf{x}} = \begin{bmatrix} \mathbf{0} & \mathbf{I} \\ -\mathbf{\Omega} & -\mathbf{\Delta} \end{bmatrix}\mathbf{x} + \begin{bmatrix} \mathbf{0} \\ \mathbf{\Phi}^{\mathrm{T}}\bar{\mathbf{B}} \end{bmatrix}\mathbf{u}(t) + \begin{bmatrix} \mathbf{0} \\ \mathbf{\Phi}^{\mathrm{T}}\bar{\mathbf{E}} \end{bmatrix}\mathbf{f}(t) \tag{7}$$

where $\mathbf{x}(t) = \begin{bmatrix} \mathbf{z} & \dot{\mathbf{z}} \end{bmatrix}^{\mathrm{T}}$ represents a state-space vector. With the state and the output equations, the state space model is represented in the form:

$$\dot{\mathbf{x}}(t) = \mathbf{A}\mathbf{x}(t) + \mathbf{B}\mathbf{u}(t) + \mathbf{E}\mathbf{f}(t), \quad \mathbf{y} = \mathbf{C}\mathbf{x}(t) + \mathbf{D}\mathbf{u}(t) + \mathbf{F}\mathbf{f}(t) \tag{8}$$

which is convenient for the controller design.

4. Subspace-Based System Identification

As an alternative modeling method, the subspace-based system identification can be used. It is convenient for the comparison with the results of the state space FEA-based modeling, since it results in a state space model representation as well. Based on the measured input and output signal data, the model is identified in a discrete-time state-space form, which represents a discrete-time equivalent of the state space model given by (8). In a general case a deterministic-stochastic form of a discrete-time state-space model has the following form:

$$\mathbf{x}[k+1] = \mathbf{\Phi}\mathbf{x}[k] + \mathbf{\Gamma}\mathbf{u}[k] + \boldsymbol{w}[k], \qquad \mathbf{y}[k] = \mathbf{C}\mathbf{x}[k] + \mathbf{D}\mathbf{u}[k] + \boldsymbol{v}[k] \tag{9}$$

with discrete-time state and control matrices $\mathbf{\Phi}$ and $\mathbf{\Gamma}$, and the process and the measurement noise $\boldsymbol{w}[k]$ and $\boldsymbol{v}[k]$, respectively. The process noise and the measurement noise vector sequences $\boldsymbol{w}[k]$ and $\boldsymbol{v}[k]$ are white noise with zero mean and with covariance matrix:

$$\mathcal{E}\left\{\begin{bmatrix} \boldsymbol{w}[i] \\ \boldsymbol{v}[j] \end{bmatrix}\begin{bmatrix} \boldsymbol{w}[i]^{\mathrm{T}} & \boldsymbol{v}[j]^{\mathrm{T}} \end{bmatrix}\right\} = \begin{bmatrix} \mathbf{Q} & \mathbf{S} \\ \mathbf{S}^{\mathrm{T}} & \mathbf{R} \end{bmatrix} \tag{10}$$

General deterministic-stochastic problem of the subspace identification is to determine the order n of the unknown system and the system matrices $\mathbf{\Phi} \in \mathrm{R}^{n\times n}$, $\mathbf{\Gamma} \in \mathrm{R}^{n\times m}$, $\mathbf{C} \in \mathrm{R}^{l\times n}$, $\mathbf{D} \in \mathrm{R}^{l\times m}$ as well as the covariance matrices $\mathbf{Q} \in \mathrm{R}^{n\times n}$, $\mathbf{S} \in \mathrm{R}^{n\times l}$, $\mathbf{R} \in \mathrm{R}^{l\times l}$ of the noise sequences $\boldsymbol{w}[k]$ and $\boldsymbol{v}[k]$. Subsequent derivations regard the pure deterministic case considered in [4].

Measured input and output data are organized into block Hankel matrices defined in the following form [13, 15, 19]:

$$U_{0|2i-1} \overset{def}{=} \left[\begin{array}{ccccc} \mathbf{u}_0 & \mathbf{u}_1 & \mathbf{u}_2 & \cdots & \mathbf{u}_{j-1} \\ \mathbf{u}_1 & \mathbf{u}_2 & \mathbf{u}_3 & \cdots & \mathbf{u}_j \\ \cdots & \cdots & \cdots & \cdots & \cdots \\ \mathbf{u}_{i-1} & \mathbf{u}_i & \mathbf{u}_{i+1} & \cdots & \mathbf{u}_{i+j-2} \\ \hline \mathbf{u}_i & \mathbf{u}_{i+1} & \mathbf{u}_{i+2} & \cdots & \mathbf{u}_{i+j-1} \\ \mathbf{u}_{i+1} & \mathbf{u}_{i+2} & \mathbf{u}_{i+3} & \cdots & \mathbf{u}_{i+j} \\ \cdots & \cdots & \cdots & \cdots & \cdots \\ \mathbf{u}_{2i-1} & \mathbf{u}_{2i} & \mathbf{u}_{2i+1} & \cdots & \mathbf{u}_{2i+j-2} \end{array}\right] \tag{11}$$

The output block Hankel matrix $Y_{0|2i-1}$ is defined in a similar way. More details on definition of the Hankel matrices and the subspace-based identification method can be found in [15]. The measurement data are organized in the form of the input-output relation [19]:

$$\mathbf{Y}[k] = \mathbf{\Gamma}_\alpha \mathbf{x}[k] + \mathbf{\Phi}_\alpha \mathbf{U}[k] \tag{12}$$

where $\mathbf{\Gamma}_\alpha$ represents the observability matrix for the system (1), $\mathbf{\Phi}_\alpha$ is the Toeplitz matrix [4] of impulse responses from **u** to **y**:

$$\mathbf{\Phi}_\alpha = \begin{bmatrix} \mathbf{D} & 0 & \cdots & \mathbf{0} \\ \mathbf{C\Gamma} & \mathbf{D} & & \mathbf{0} \\ \vdots & \ddots & \ddots & \vdots \\ \mathbf{C\Phi}^{\alpha-2}\mathbf{\Gamma} & \cdots & \mathbf{C\Gamma} & \mathbf{D} \end{bmatrix} \tag{13}$$

and α is a specified number greater than the state dimension but much smaller than the data length. For a deterministic case [13] the problem is simplified to determining $\mathbf{\Gamma}_\alpha$ and $\mathbf{\Phi}_\alpha$ by computing the singular value decomposition (SVD) of **U** in the first step:

$$\mathbf{U} = \mathbf{P\Sigma Q}^{\mathrm{T}} = [\mathbf{P}_{u1} \quad \mathbf{P}_{u2}] \begin{bmatrix} \mathbf{\Sigma}_u & 0 \end{bmatrix} \begin{bmatrix} \mathbf{Q}_{u1}^{\mathrm{T}} \\ \mathbf{Q}_{u2}^{\mathrm{T}} \end{bmatrix}. \tag{14}$$

If matrix **U** has dimension $m\times n$ and rank r, then the partition in (14) is performed as follows:

$$\mathbf{P} = \left[\mathbf{p}_1 \quad \cdots \quad \mathbf{p}_r \mid \mathbf{p}_{r+1} \quad \cdots \quad \mathbf{p}_m\right] = \left[\mathbf{P}_{u1} \quad \mathbf{P}_{u2}\right] \tag{15}$$

$$\mathbf{Q} = \begin{bmatrix} \mathbf{q}_1 & \cdots & \mathbf{q}_r & | & \mathbf{q}_{r+1} & \cdots & \mathbf{q}_n \end{bmatrix} = \begin{bmatrix} \mathbf{Q}_{u1} & \mathbf{Q}_{u2} \end{bmatrix} \tag{16}$$

where $\mathbf{p}_i$ are the left singular vectors of $\mathbf{U}$ [4]. It can be shown that they are eigenvectors of $\mathbf{U}\mathbf{U}^{\mathrm{T}}$. Vectors $\mathbf{q}_i$ are the right singular vectors of $\mathbf{U}$. It can be shown that they are eigenvectors of $\mathbf{U}^{\mathrm{T}}\mathbf{U}$. Multiplying (12) by $\mathbf{Q}_{u2}$, matrix $\boldsymbol{\Gamma}_\alpha$ can be determined from a SVD of $\mathbf{Y}\mathbf{Q}_{u2}$. Then matrix $\mathbf{C}$ is obtained as the first row (in a sense of a block-row) of the observability matrix $\boldsymbol{\Gamma}_\alpha$, and matrix $\boldsymbol{\Phi}$ is calculated from: $\underline{\boldsymbol{\Gamma}}_\alpha = \overline{\boldsymbol{\Gamma}}_\alpha \boldsymbol{\Phi}$ applying pseudo inverse, where $\overline{\boldsymbol{\Gamma}}_\alpha$ is obtained by dropping the last row of $\boldsymbol{\Gamma}_\alpha$. Matrix $\underline{\boldsymbol{\Gamma}}_\alpha$ represents the matrix obtained by dropping the first row of $\boldsymbol{\Gamma}_\alpha$. For the calculation of $\boldsymbol{\Gamma}$ and $\mathbf{D}$ matrices, (12) is multiplied by the pseudo inverse of $\mathbf{U}$ on the right and by $\mathbf{P}_{u2}^{\mathrm{T}}$ from (14) on the left. Thus the equation is reduced to:

$$\mathbf{P}_{u2}^{\mathrm{T}} \mathbf{Y} \mathbf{U}^{-1} = \mathbf{P}_{u2}^{\mathrm{T}} \boldsymbol{\Phi}_\alpha \,. \tag{17}$$

After rearranging, (17) can be solved for $\boldsymbol{\Gamma}$ and $\mathbf{D}$ using the least squares, see (13). In this way the system parameters in the form of state-space matrices of the model (9) are identified using the subspace-based identification method.

5. Optimal LQ Controller Design with Additional Dynamics

An optimal LQ controller design with additional dynamics is suggested here as a control technique which has resulted in a successful vibration and noise reduction in several studies [12, 16].

Controller design includes available a priori knowledge about occurring disturbance type contained in the additional dynamics. Such an a priori knowledge is available in terms of the type of the disturbance function which has to be rejected or whose influence should be suppressed by the controller. Periodic disturbances with frequencies corresponding to the eigenfrequencies of the smart structure can cause resonance and their suppression is therefore important. They are taken into account via the additional dynamics.

Discrete-time state space equivalent (18) of the state space model (8) developed through the FEM procedure and modal reduction is used for the controller design.

$$\mathbf{x}[k+1] = \boldsymbol{\Phi}\mathbf{x}[k] + \boldsymbol{\Gamma}\mathbf{u}[k] + \boldsymbol{\varepsilon}\mathbf{w}[k], \qquad \mathbf{y}[k] = \mathbf{C}\mathbf{x}[k] + \mathbf{D}\mathbf{u}[k] + \mathbf{F}\mathbf{w}[k] \tag{18}$$

Using the a priori knowledge about the disturbance class, which has to be suppressed, the model of the disturbance is represented in an appropriate state space form, where the disturbance is assumed to be the output of the state space representation. The poles λ_i of the disturbance transfer function are used to define the additional dynamics using the coefficients of the polynomial:

$$\delta(z) = \prod_i (z - \mathrm{e}^{\lambda_i T})^{m_i} = z^s + \delta_1 z^{s-1} + \ldots + \delta_s \tag{19}$$

where m_i represents the multiplicity of the pole λ_i. Additional dynamics is expressed in a state space form:

$$\mathbf{x}_a[k+1] = \mathbf{\Phi}_a \mathbf{x}_a[k] + \mathbf{\Gamma}_a \mathbf{e}[k]\,; \tag{20}$$

where $\mathbf{x}_a$ is the vector of the state variables for the additional dynamics, $\mathbf{e}$ is the error signal and:

$$\mathbf{\Phi}_a = \begin{bmatrix} -\delta_1 & 1 & 0 & \cdots & 0 \\ -\delta_2 & 0 & 1 & \cdots & 0 \\ \vdots & \vdots & \vdots & \ddots & \vdots \\ -\delta_{s-1} & 0 & 0 & \cdots & 1 \\ -\delta_s & 0 & 0 & \cdots & 0 \end{bmatrix}, \quad \mathbf{\Gamma}_a = \begin{bmatrix} -\delta_1 \\ -\delta_2 \\ \vdots \\ -\delta_{s-1} \\ -\delta_s \end{bmatrix}. \tag{21}$$

For multiple-input multiple-output (MIMO) systems additional dynamics is replicated q times (once per each output). Replicated additional dynamics is described by:

$$\bar{\mathbf{\Phi}} \overset{def}{=} diag(\underbrace{\mathbf{\Phi}_a, ..., \mathbf{\Phi}_a}_{q \text{ times}}), \quad \bar{\mathbf{\Gamma}} \overset{def}{=} diag(\underbrace{\mathbf{\Gamma}_a, ..., \mathbf{\Gamma}_a}_{q \text{ times}}) \tag{22}$$

The discrete-time design model ($\mathbf{\Phi}_d$, $\mathbf{\Gamma}_d$) is formed as a cascade combination of the additional dynamics ($\mathbf{\Phi}_a$, $\mathbf{\Gamma}_a$) or $(\bar{\mathbf{\Phi}}, \bar{\mathbf{\Gamma}})$ and the discrete-time plant model ($\mathbf{\Phi}$, $\mathbf{\Gamma}$):

$$\mathbf{x}_d[k+1] = \mathbf{\Phi}_d \mathbf{x}_d[k] + \mathbf{\Gamma}_d \mathbf{u}[k]\,; \tag{23}$$

$$\mathbf{\Phi}_d = \begin{bmatrix} \mathbf{\Phi} & \mathbf{0} \\ \mathbf{\Gamma}^* \mathbf{C} & \mathbf{\Phi}^* \end{bmatrix}, \mathbf{\Gamma}_d = \begin{bmatrix} \mathbf{\Gamma} \\ \mathbf{0} \end{bmatrix}, \ \mathbf{x}_d = \begin{bmatrix} \mathbf{x}[k] \\ \mathbf{x}_a[k] \end{bmatrix} \tag{24}$$

where $\mathbf{\Phi}^*$ and $\mathbf{\Gamma}^*$ denote respectively $\mathbf{\Phi}_a$ and $\mathbf{\Gamma}_a$ in the case of single-input single-output systems or $\bar{\mathbf{\Phi}}$ and $\bar{\mathbf{\Gamma}}$ for MIMO systems. For the design model (23) the feedback gain matrix $\mathbf{L}$ of the optimal LQ regulator is calculated in such a way that the feedback control law $\mathbf{u}[k] = -\mathbf{L}\mathbf{x}_d[k]$ minimizes the performance index (25) subject to the constraint (23), where $\mathbf{Q}$ and $\mathbf{R}$ are symmetric, positive-definite matrices.

$$J = \frac{1}{2} \sum_{k=0}^{\infty} (\mathbf{x}_d[k]^T \mathbf{Q} \mathbf{x}_d[k] + \mathbf{u}[k]^T \mathbf{R} \mathbf{u}[k]) \tag{25}$$

The feedback gain matrix $\mathbf{L}$ is afterwards partitioned into

$$\mathbf{L} = \begin{bmatrix} \mathbf{L}_1 & \mathbf{L}_2 \end{bmatrix} \tag{26}$$

so that $\mathbf{L}_1$ corresponds to the state space model of the structure, and $\mathbf{L}_2$ to the modelled additional dynamics.

6. Direct Adaptive Control

As an alternative approach, the model reference adaptive control (MRAC) is suggested. This control technique comprises several advantages for the large flexible structures. In the case of piezoelectric smart structures the term large can regard high

number of degrees of freedom of the finite element model used for the modeling of the structure behavior. With the model truncation, which is a necessary step to adapt the structure model to the controller design purpose, resulting state-space model does not exactly reflect the real behavior of the structure. Inaccuracies introduced in this way can be viewed as a source of the parameter variation with respect to the modeled case. The presence of disturbances in real environment also introduces variation of the parameters in comparison with the modeled case. This causes the need for the adaptive control algorithm, which can successfully face the insufficient prior knowledge or the unknown changes of the system parameters.

The advantage of a robust adaptive controller over a fixed-gain controller can be viewed through the fact that in design of large flexible smart structures a large degree of the model uncertainty is allowable in the sense of the possible parameter variation as well as with respect to the order of the controlled structure. The robustness assumes stability in the presence of disturbances and unmodeled dynamics.

The idea of the model reference adaptive control is based upon the existence of the reference model, specified by the designer, which reflects the desired behavior of the controlled structure. The output of the controlled structure should track the output of the reference model (Fig. 7).

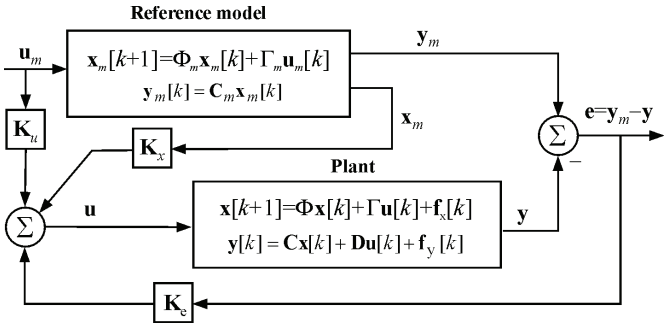

Fig. 7 General form of a discrete-time MRAC system

A general form of a discrete-time model reference adaptive system is represented in Fig. 7. Plant representation is a discrete-time state space realization, which corresponds to the plant model (18), whereas the reference model is represented by equations in Fig. 7, where $\mathbf{f}_x$ and $\mathbf{f}_y$ represent bounded unmeasurable plant and output disturbances in a general case and $\mathbf{e}=\mathbf{e}_y$ is the output error, i.e. the difference between the desired output of the reference model and the real plant output.

Discrete-time direct model reference adaptive control law is expressed in the following form:

$$\mathbf{u}[k]=\mathbf{K}_r[k]\mathbf{r}[k]=\mathbf{K}_e[k]\mathbf{e}_y[k]+\mathbf{K}_x[k]\mathbf{x}_m[k]+\mathbf{K}_u[k]\mathbf{u}_m[k]. \tag{27}$$

The adaptive gain $\mathbf{K}_r[k]$ in is determined as a sum of proportional and integral parts $\mathbf{K}_p$ and $\mathbf{K}_I$ respectively:

$$\mathbf{K}_r[k]=\mathbf{K}_p[k]+\mathbf{K}_I[k] \tag{28}$$

According to the basic model reference adaptive algorithm the proportional and integral gains are adapted in the following way:

$$\mathbf{K}_p[k] = \mathbf{e}_y \mathbf{r}^T(t)\bar{\mathbf{T}}, \quad \mathbf{K}_I[k+1] = \mathbf{e}_y \mathbf{r}^T[k]\mathbf{T}, \quad \mathbf{K}_I(0) = \mathbf{K}_{I0} \tag{29}$$

where $\mathbf{T}$ and $\bar{\mathbf{T}}$ are $n_r \times n_r$ time-invariant weighting matrices and $\mathbf{K}_{I0}$ is the initial integral gain, selected by the designer. In the robust model reference adaptive control approach the integral gain is determined in the form (30). This modification of the integral gain in (29) by adding a σ-term is introduced to provide the convergence of the integral gain [14] since in realistic environment due to disturbances the error **e** does not reach the zero value and the integral gain would thus never stop increasing without its limiting by the σ-term.

$$\mathbf{K}_I[k+1] = \mathbf{e}_y[k]\mathbf{r}^T[k]\mathbf{T} - \sigma\mathbf{K}_I[k] \tag{30}$$

The control law for a general plant in Fig. 7 including disturbances or excitations is globally stable with respect to boundness if the disturbances are bounded and the plant is is almost strictly positive real. The proof of the condition is based on the selection of the Lyapunov candidate positive definite function and on analyzing the sign of its derivative. In order to guarantee robust stability, perfect tracking is not obtained in general, but the adaptive controller maintains a small tracking error over large ranges of nonideal conditions and uncertainties.

7. Application Examples

In order to illustrate some results of the application of active control as a part of the overall design of active mechanical structures several examples are shown in this section.

7.1. Active vibration suppression of a car roof

Fig. 8 Passenger compartment and inner surface of the car roof with attached piezo-patches and exciting shakers

Vibration suppression of a car roof with attached piezoelectric patches using the optimal LQ controller with additional dynamics is demonstrated through a numerical simulation for a test structure. Piezoelectric patches attached to the surface of the car roof are used as actuators and sensors. Excitation by shakers at prescribed points is intended for the experimental investigations (Fig. 8).

FEM model including the piezo-electric effects of the actuator/sensor groups was obtained using the FEM software COSAR [3]. Based on the generated FEM mesh, an optimization

of the actuator/sensor placement was per-formed under consideration of the eigen-modes of interest and the controllability index. The actuator/sensor placement in Fig. 9 describes one of the test cases, which was calculated based on the controllability index. Comparison of the calculated an experimentally determined eigenfrequencies shows a good agreement in the considered frequency range.

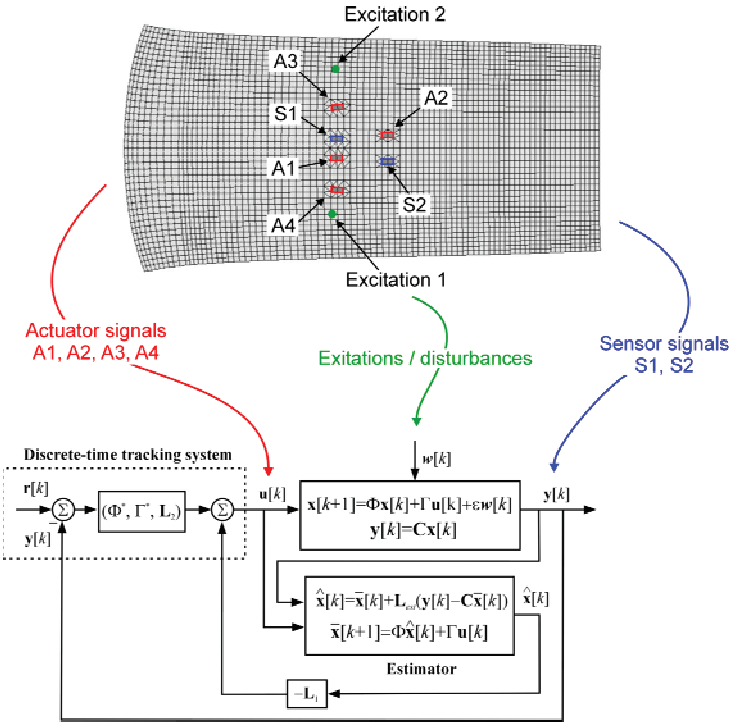

Fig. 9 FEM mesh of the car roof with actuator/sensor placement

For the controller design a modally reduced state space model was used, which takes into account five selected eigenfrequencies: f_1=48.45Hz, f_2=51.12Hz, f_3=63.23Hz, f_4=64.67Hz and f_5=68.00Hz. Using the control concept with optimal LQ controller, additional dynamics and Kalman estimator the simulation of the vibration suppression was performed in order to show the potentials of the control strategy. The results are represented in Fig. 10.

The comparison of the uncontrolled and controlled cases shows significant reduction of the vibration magnitudes in the presence of the controller. The controller was also compared with the standard optimal LQ controller without additional dynamics which compensates for the presence of the periodic sinusoidal excitations with critical frequencies. The comparison shows much better vibration suppression in the presence of the controller with additional dynamics.

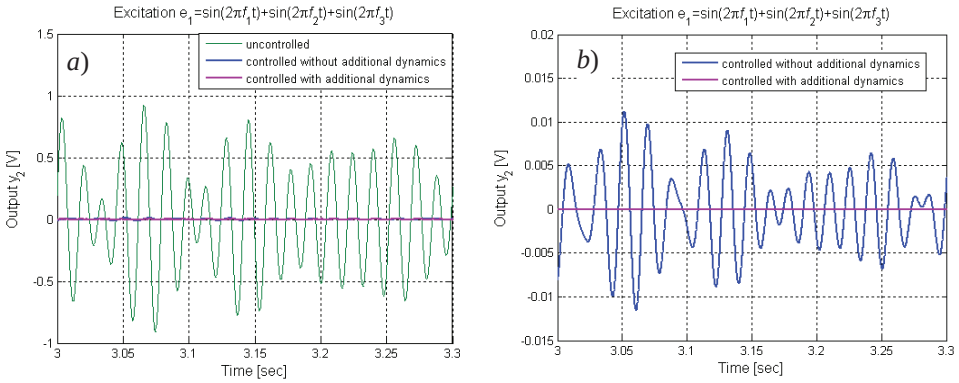

Fig. 10 *a*) Controlled and uncontrolled responses of the sensor patches.
b) Zoomed portion of the controlled responses.

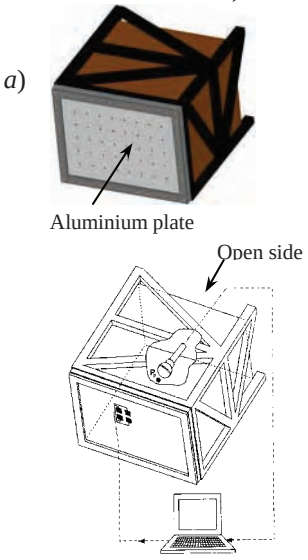

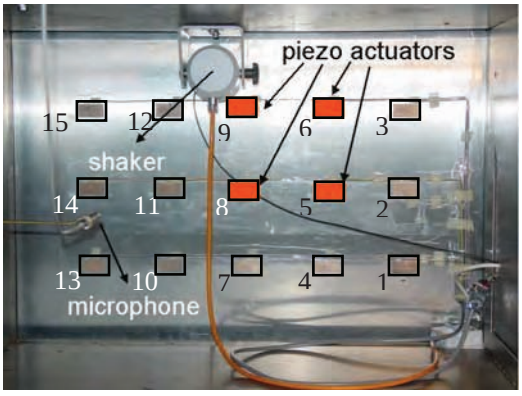

Fig. 11 *a*) Scheme of the acoustic box
b) photo of the clamped plate with piezo-actuators

7.2. Noise Control of a Smart Acoustic Box

An actively controlled smart acoustic box consisting of the clamped plate with attached piezoelectirc patches used as actuators and of the wooden box surrounding the clamped plate is designed and investigated in order to reduce the plate vibrations and the air pressure at selected points inside the box (Fig. 11).

The plate is excited by a shaker and the plate and the acoustic fluid vibrations are measured by the laser scanning vibrometer (for the velocity and displacement measurements at selected points on the plate surface) and the microphone (for the air pressure measurement) respectively. The piezopatches and the microphone are located inside the acoustic box.

The aluminium plate of the acoustic box and the acoustic fluid inside it are modelled using the FEM approach, taking into consideration the acoustic behaviour via the appropriate acoustic finite elements. Based on the modally reduced state space model obtained through the modal truncation, the simulation and subsequently the experimental control of the plate vibration and of the fluid pressure were performed using the optimal LQ controller with additional dynamics and the model reference adaptive control.

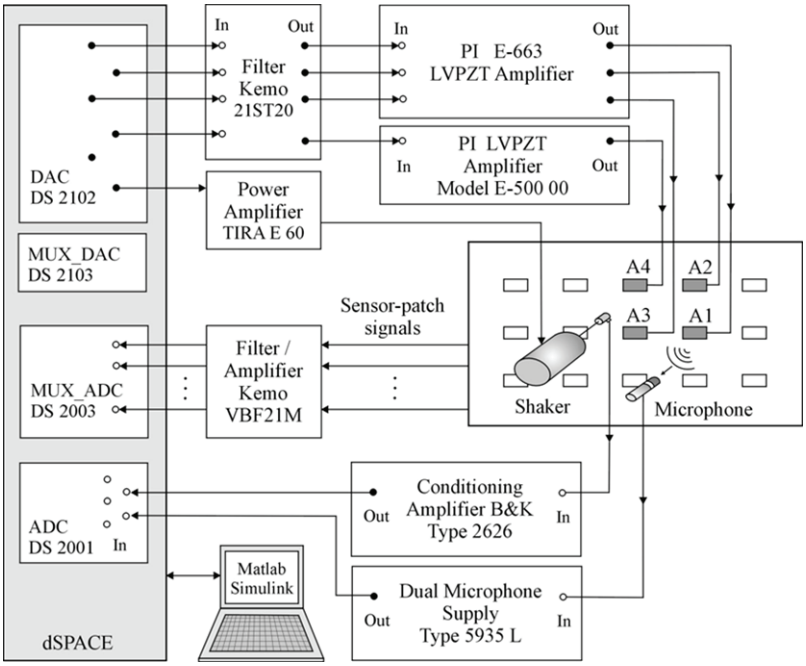

Fig. 12 Experimental setup for system identification and control implementation

The experimental setup for the control implementation as well as for the model identification using the subspace approach described in section 4 is represented in Fig. 12.

The optimal LQ controller was tested with different excitation signals. Some of the results are represented in with Fig. 13. The results for the excitation obtained as a sum of three periodic sinusoidal signals with the frequencies corresponding to the eigenfrequencies of the plate (f_{w1}=66.7Hz, f_{w2}=106.2Hz, f_{w2}=163.8Hz) are shown in Fig. 13 *a*). Fig. 13 *b*) shows the results with the random excitation signal. The pressure amplitude reduction can be observed in both cases.

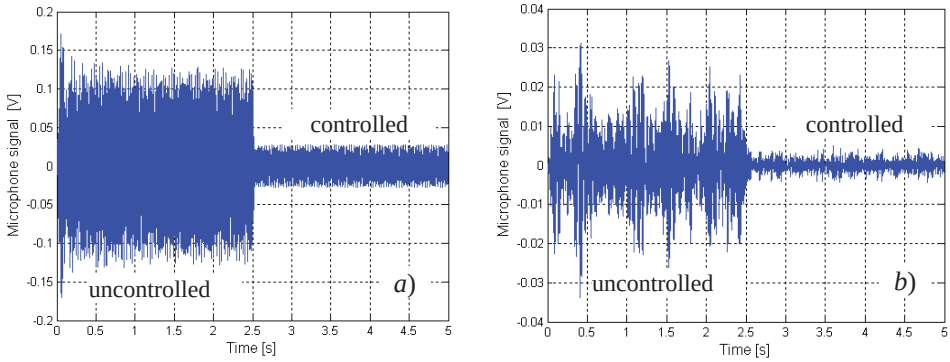

Fig. 13 Optimal LQ controller with additional dynamics: uncontrolled and controlled microphone output signal in the presence of

a) excitation $\sum_{i=1}^{3}\sin(f_{wi})$, *b*) random excitation.

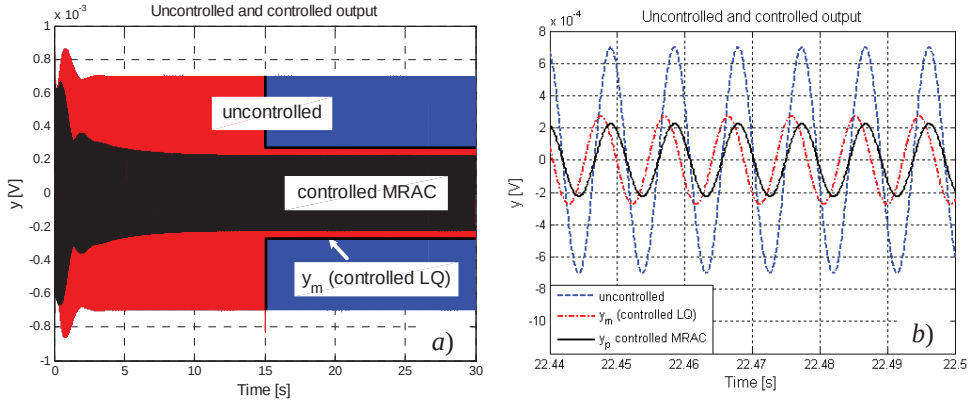

Fig. 14 *a*) Comparison of the MRAC and optimal LQ controller; *b*) zoomed portion.

The results of the adaptive MRAC controller testing are shown in Fig. 14. The adaptive controller is compared with the optimal LQ controller in the presence of the periodic excitation with the frequency f_{w2}. Uncontrolled and controlled signals are represented in Fig. 14 *a*), and a zoomed portion of the signals in Fig. 14 *b*). Both controllers perform the air pressure reduction at the microphone point. In this case the optimal controller performs a slightly higher reduction degree.

8. Conclusion

Active structural design is addressed in this paper considering several phases in the overall design approach, with the focus on structural control of lightweight mechanical

structures which use piezoelectric materials as active elements. The main control objective is vibration suppression and the noise attenuation. The feasibility of the approaches is demonstrated by two application examples: vibration suppression of the car roof and the noise reduction in a smart acoustic enclosure. Experience in the education is addressed as well. A benchmark example of a clamped beam controlled by piezoelectric patches used as actuators and/or sensors is explained to show the application possibilities for education purposes.

Acknowledgement: *A special thanks goes to Prof. Katica (Stevanović) Hedrih for invitation to participation at the symposium Address to Mechanics: Science, Teaching and Applications. The author is especially grateful for all the support Prof. Hedrih has provided. Her very helpful suggestions and advices are truly appreciated.*

REFERENCES

1. Allik H., Hughes J. R., (1970), Finite Element Method for Piezoelectric Vibration, *International Journal for Numerical Methods in Engineering*, 2:151–157
2. Berger H., Köppe H., Gabbert U., Seeger F., (2000) On Finite Element Analysis of Piezoelectric Controlled Smart Structures, (2000) *IUTAM Symposium on Smart Structures and Structronic Systems*, Proceedings of the IUTAM Symposium held in Magdeburg, Germany, 26-29 September 2000, Edited by: U. Gabbert, H. S. Tzou, 189-196
3. COSAR General Purpose Finite Element Package: Manual, FEMCOS mbH Magdeburg, http://www.femcos.de
4. Franklin G. F., Powell J. D., Workman M. L., Digital Control of Dynamic Systems, third edition, Addison-Wesley Longman, Inc., 1998
5. Gabbert U., Berger H., Köppe H., Cao X., (2000), On Modeling and Analysis of Piezoelectric smart Structures by the Finite Element Method, *Applied Mechanics and Engineering*, 5(1), 127-142
6. Gabbert U., Köppe H., Fuchs K., Seeger F., (2000), Modeling of Smart Composites Controlled by Thin Piezoelectric Fibers, in Varadan, V.V. (Ed.): *Mathematics and Control in Smart Structures*, SPIE Proceedings Series, Vol. 3984, 2-11
7. Gabbert U., Tzou H. S. (Eds.), (2001), *Smart Structures and Structronic Systems*, Dordrecht: Kluwer Academic Publisher
8. Gabbert U., Weber C. T., (1999), Analysis and Optimal Design of Piezoelectric Smart Structures by the Finite Element Method, *ECCM'99 European Conference on Computational Mechanics*, August 31 - September 3, 1999, München, Germany
9. Janocha H. (Ed.), (2007), *Adaptronics and Smart Structures – Basics, Materials, Design, and Applications*, 2nd ed., Springer Verlag
10. Laugwitz F., Lefèvre J., Schmidt G., Nestorović T., Gabbert U., (2006), Experimental and numerical investigation of a smart acoustic box, *ISMA2006 International Conference on Noise and Vibration Engineering*, September 18-20, 2006, Katholieke Universiteit Leuven, Belgium

11. Lefèvre J., Gabbert U., (2005), Finite Element Modelling of Vibro-Acoustic Systems for Active Noise Reduction, *Technische Mechanik*, 25 (3-4), 241–247
12. Nestorović T., (2005), *Controller Design for the Vibration Suppression of Smart Structures*, Fortschritt-Berichte VDI, 8(1071), Düsseldorf
13. Nestorović T., H. Köppe, U. Gabbert, (2005), Subspace Identification for the model based controller design of a funnel-shaped structure, *Facta Universitatis, Series Mechanics, Automatic Control and Robotics*, 4(17), 257–263
14. Nestorović Trajkov T., Köppe H., Gabbert U., (2008), Direct model reference adaptive control (MRAC) design and simulation for the vibration suppression of piezoelectric smart structures, *Communications in Nonlinear Science and Numerical Simulation*, 13(9), 1896-1909
15. Nestorović-Trajkov T., Gabbert U., (2006), Active control of a piezoelectric funnel-shaped structure based on subspace identification, *Structural Control and Health Monitoring*, 13(6), 1068–1079
16. Nestorović-Trajkov T., Köppe H., Gabbert U., (2005), Active Vibration Control Using Optimal LQ Tracking System with Additional Dynamics, *International Journal of Control*, 78(15), 1182–1197
17. Tiersten H.F., (1967), Hamilton's principle for linear piezoelectric media, *Proc. IEEE*, 1523–1524
18. Tzou H. S., Tseng C. I., (1990), Distributed piezoelectric sensor/actuator design for dynamic measurement/ control of distributed parameter system: a piezoelectric finite element approach, *Journal of Sound and Vibration*, 138(1), 17–34
19. Van Overschee P., De Moor B., (1996), *Subspace Identification for Linear Systems: Theory, Implementation, Applications*, Kluwer Academic Publishers, Boston

AKTIVNO UPRAVLJANJE KONSTRUKCIJAMA U ISTRAŽIVANJU I NASTAVI

Prof. Dr.-Ing. Tamara Nestorović

U ovom radu prikazane su ključne faze u sveobuhvatnom pristupu projektovanju aktivnih konstrukcija. Težište rada je na upravljanju lakih i tankozidnih mehaničkih struktura u cilju aktivne redukcije vibracija i smanjenja nivoa emitovane buke primenom piezoelektričnih aktuatora i senzora. Rastuće interesovanje za razvoj aktivnih konstrukcija kao i iskustva u istraživanju motivisali su uvođenje predmeta o aktivnim konstrukcijama u nastavu na univerzitetima. Ove oblasti se intenzivno izučavaju u nastavi i nailaze na veliko interesovanje među studentima. U radu se takođe navode i iskustva autora na polju nastave u ovoj oblasti.

Ključne reči: *upravljanje aktivnim konstrukcijama, piezoelektrični actuatori i senzori, identifikacija sistema.*

Submitted on April 2009, accepted on June 2012

DOI : 10.2298/TAM12S1203N Math.Subj.Class.: 93C40; 93B03; 93C10; 74S05;